










## Article

# Spatial Modelling of Soil Quality Index Using Regression–Kriging and Delineation of Nutrient Management Zones in High-Andean Quinoa Fields, Southern Peru

Nestor Cuellar-Condori <sup>1</sup>, Sharon Mejia <sup>2</sup>, Robert Quiñones <sup>2</sup>, Ruth Mercado <sup>2</sup>, Ali Cristhian <sup>1</sup>,  
Karla Chávez-Zea <sup>1</sup>, Elvis Ccosi <sup>1</sup>, Madeleiny Cahuide <sup>3</sup> and Kenyi Quispe <sup>2,\*</sup>

<sup>1</sup> Dirección de Servicios Estratégicos Agrarios, Instituto Nacional de Innovación Agraria (INIA), Av. Industrial 26, Rinconada de Salcedo, Puno 21001, Peru; 20110700@lamolina.edu.pe (N.C.-C.)

<sup>2</sup> Dirección de Servicios Estratégicos Agrarios, Instituto Nacional de Innovación Agraria (INIA), Av. La Molina 1981, Lima 15024, Peru; sharon.mejia.m29@gmail.com (S.M.); robert.quino14@gmail.com (R.Q.); ruth.mercado76@gmail.com (R.M.)

<sup>3</sup> Escuela de Posgrado, Maestría en Desarrollo Rural, Universidad Nacional del Altiplano, Avenida Sesquicentenario #1153, Puno 21127, Peru

\* Correspondence: investigacion\_labsaf@inia.gob.pe

## Abstract

The pronounced heterogeneity of high-Andean soils constitutes a critical constraint to the sustainable productivity of quinoa in southern Peru, where current yields ( $1.6 \text{ t ha}^{-1}$ ) remain well below potential ( $>5 \text{ t ha}^{-1}$ ). This study aimed to develop a spatially predictive model of a weighted soil quality index (SQIw), the edaphic supply of nitrogen (N), phosphorus (P) and potassium (K), and the agricultural gypsum requirement by integrating edaphoclimatic covariates through regression–kriging. A total of 198 quinoa-cultivated soil samples were analysed; a minimum data set (MDS) was defined using correlation and principal component analyses, and regression–kriging was applied to map SQIw and the variables of interest. The MDS comprised electrical conductivity (EC), organic matter (OM), available P, exchangeable Na, sand, clay, and effective cation exchange capacity (ECEC); exchangeable Na ( $W_i = 0.160$ ) and available P ( $W_i = 0.158$ ) received the largest weights in the SQIw. SQIw values ranged from 0.22 to 0.84 and supported a five-class soil quality taxonomy; spatial modelling revealed a dominance of moderate-quality soils across the territory (85.21% of the agricultural area, 13,461.19 ha). The model achieved  $R^2 = 0.56$ , RMSE = 0.05, and MAE = 0.04 for SQIw. Most of the area (12,175.65 ha; 77%) exhibited an intermediate gypsum requirement ( $9.73\text{--}14.33 \text{ t ha}^{-1}$ ). Nitrogen and phosphorus showed the greatest territorial limitations, whereas potassium was largely non-limiting ( $84.82\text{--}570.17 \text{ kg ha}^{-1}$ ). These results indicate that sodicity and N–P deficiencies are the primary functional constraints; the generated maps enable prioritisation of gypsum amendments and targeted variable-rate fertilisation strategies to optimise the sustainability of quinoa production in the Altiplano.



Academic Editors: Marco Acutis and Baohua Zhang

Received: 10 December 2025

Revised: 26 February 2026

Accepted: 18 March 2026

Published: 24 March 2026

Copyright: © 2026 by the authors.

Licensee MDPI, Basel, Switzerland.

This article is an open access article distributed under the terms and conditions of the [Creative Commons Attribution \(CC BY\) license](https://creativecommons.org/licenses/by/4.0/).

**Keywords:** spatial soil mapping; high-andean soils; variable-rate fertilisation; gypsum requirement

## 1. Introduction

The sustainability of agricultural systems in the high-Andean ecosystems of southern Peru is challenged by strong edaphic variability, harsh climatic conditions, and limited soil-management technologies [1]. In this setting, quinoa (*Chenopodium quinoa* Willd.), a native Andean pseudocereal, is a key agricultural and nutritional resource due to its

remarkable tolerance to extreme environments and high dietary value [2,3]. However, nutrient availability and the physicochemical properties of soils—highly heterogeneous in mountainous landscapes—directly shape grain production and quality.

Quinoa is economically and culturally important across the region. Over the past decade, cultivated area has remained between 33,296 and 34,167 ha, while production rose from 38,220 t to 41,958 t in 2024, driven by yield increases from 1.12 to 1.26 t ha<sup>-1</sup>; some 56,322 families currently depend on quinoa production [4]. Given the crop's ability to persist in marginal environments, characterising the spatial variability of soil properties and the crop's nutrient requirements is essential to improve productivity in high-Andean agroecosystems [5,6].

Integrating soil analyses with environmental predictors derived from geographic information systems enables advanced geostatistical approaches such as regression-kriging, which combines deterministic models with the spatial structure of residual variation [7]. In recent years, RK has been widely applied in agricultural and soil science to map nutrient availability, salinity, pH, and composite soil quality indicators, particularly in heterogeneous landscapes. Regression-kriging frequently outperforms purely deterministic or purely geostatistical methods (e.g., IDW, ordinary kriging) when auxiliary covariates are available, such as topographic, vegetation, and remote-sensing indices and climatic variables [8], and it has proven effective for delineating management zones and supporting site-specific soil management strategies [9,10]. Despite its proven utility for mapping soil properties, the application of regression-kriging for managing spatial variability of soil fertility, integrated soil quality assessment, and nutrient management in quinoa-based high-Andean agroecosystems of southern Peru remains limited, representing a clear opportunity for applied, spatially explicit research [11].

Quinoa is strategic for food security and rural development in the high Andes, yet observed field yields remain well below the crop's potential; under optimal edaphic and nutritional management, yields can exceed 6–7 t ha<sup>-1</sup> [12,13]. This productivity gap is mainly associated with soil degradation, low inherent fertility on steep slopes, and suboptimal fertiliser practices. Consequently, the economic viability and sustainability of quinoa systems hinge on fertilisation plans and amendments that are adapted to spatial variability within the landscape.

Soil quality is a robust integrative indicator of productive capacity and agro-environmental sustainability [14]. Weighted soil quality indices (SQI<sub>w</sub>) have become valuable tools for synthesising multiple soil properties and identifying edaphic limitations to crop performance [15]. However, in heterogeneous mountain landscapes, these indices must be combined with spatial modelling to guide site-specific management. Regression-kriging, by coupling multiple environmental predictors with kriging of residuals, facilitates high-resolution mapping and accurate prediction of soil quality and nutrient supply [16]. Applied to quinoa systems, this approach can delineate management zones, optimise fertiliser and amendment use, and improve the sustainability of high-Andean agriculture.

This study aims to develop a spatial predictive model of the weighted soil quality index (SQI<sub>w</sub>), the edaphic supply of nitrogen (N), phosphorus (P), potassium (K), and the agricultural gypsum requirement in soils cultivated with *Chenopodium quinoa* by integrating edaphic-climatic covariates using regression-kriging. The specific objectives are: (i) to assess the physical and chemical properties of soils under quinoa cultivation; (ii) to construct a soil quality index (SQI<sub>w</sub>) tailored to the Puno Altiplano; (iii) to delineate the spatial distribution of primary macronutrient supply (N, P, and K) and agricultural gypsum requirement according to soil quality classes; and (iv) to generate site-specific management maps to inform differentiated strategies for enhancing the productivity and sustainability of high-Andean agroecosystems.

## 2. Material and Methods

### 2.1. Study Area

The study area, located in the southern highlands of Peru, encompasses approximately 15,797.37 ha of agricultural land in the district of Cabana, San Román Province, Puno Department (Figure 1). The region lies at a mean altitude of 3901 m above sea level (m a.s.l.) and is characterised by a cold climate with dry autumn and winter seasons. Mean annual precipitation is ~650 mm; minimum temperatures range from  $-4\text{ }^{\circ}\text{C}$  to  $5\text{ }^{\circ}\text{C}$ , and maximum temperatures from  $15\text{ }^{\circ}\text{C}$  to  $18\text{ }^{\circ}\text{C}$ . The geological age of the parent material is predominantly Quaternary (90%) (Figure 2a), and the dominant soil types are Chernozems (47%) and Cambisols (46%) (Figure 2b). The life zone corresponds to the Lower Montane Humid Subtropical Forest. Historical climate averages were obtained from the WorldClim (v2020) [17].

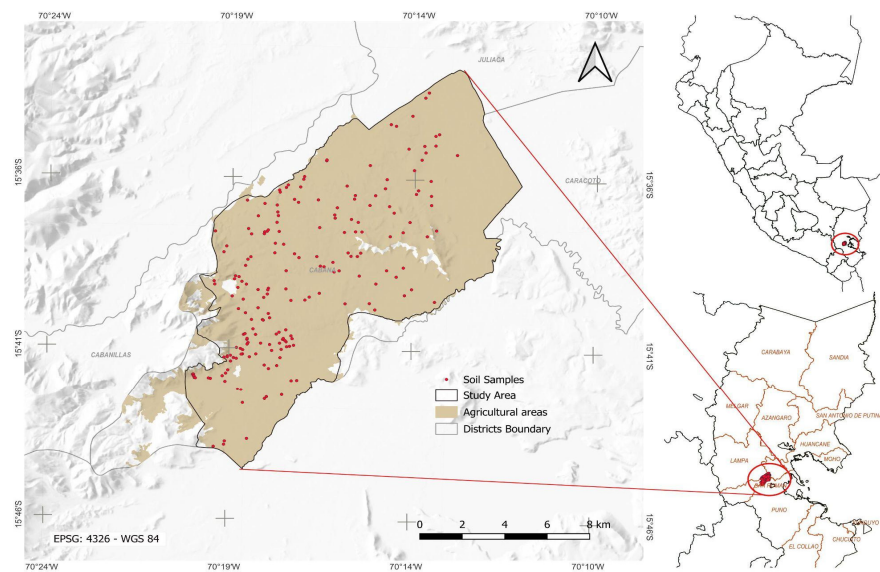


**Figure 1.** Location map with 198 sampling points in Cabana district.

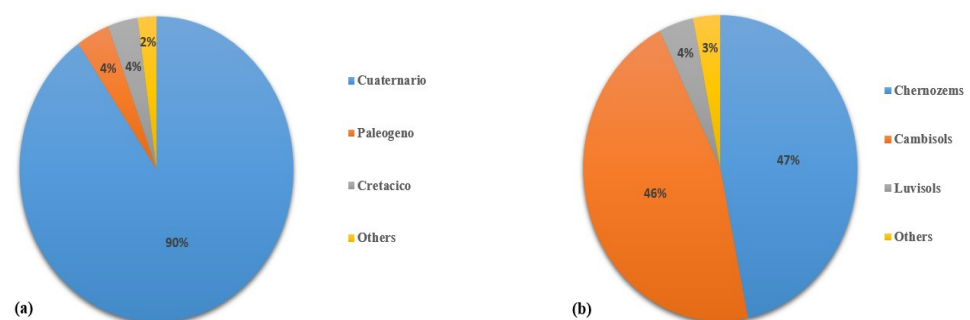


**Figure 2.** (a) Predominant type of geology in the Cabana district. (b) Soil taxonomic categories.

Quinoa cultivation represents one of the main agricultural activities in the district, with approximately 779 ha managed under organic production systems in Cabana. The cultivated area is predominantly composed of white quinoa (556.31 ha; 71.4%), followed by black quinoa (184.60 ha; 23.7%) and red quinoa (38.09 ha; 4.9%). Cañihua is also cultivated to a lesser extent.

Average quinoa yields in the area range between  $0.8$  and  $1.2\text{ t ha}^{-1}$  under rainfed conditions. Productivity is strongly influenced by edaphic constraints identified in this study, particularly soil sodicity and phosphorus deficiency. This production context underscores the relevance of developing a soil quality index adapted to quinoa-growing systems under high-Andean conditions.

## 2.2. Soil Sampling

Soil sampling followed the approach of [18]. Each sample represented a homogeneous management area ( $\leq 3$  ha), previously delineated based on slope, soil texture, and surface colour. Within each area, ten subsamples were collected at 0–30 cm depth following a zig-zag sampling pattern to capture within-field spatial variability. Subsamples were taken at regular intervals and thoroughly homogenised to obtain one composite sample representative of the management unit. Composite sampling was adopted to reduce small-scale variability and to characterise the average soil condition at the scale relevant for fertility management and spatial modelling. In total, 198 composite samples were collected across the Cabana district (Figure 1).

Sampling points were spatially distributed across the entire study area to ensure representation of the main environmental gradients. The design avoided excessive clustering and provided adequate spatial coverage for variogram estimation and regression-kriging modelling.

## 2.3. Soil Analysis

Soil samples were analysed at the Network of Soil, Water and Foliar Laboratories of the National Institute of Agrarian Innovation (LABSAF-INIA). Samples were pre-treated, air-dried at  $<40$  °C, and sieved to  $<2$  mm [19]. Soil texture was determined by the Bouyoucos hydrometer method [20]. Soil pH was measured following the standardised EPA 9045D method [21]. Electrical conductivity (EC) was measured according to [22]/Cor.1:1996. Calcium carbonate ( $\text{CaCO}_3$ ) content was determined by acid neutralisation (calcmeter) following [20]. To convert EC measured in diluted soil–water extracts to the electrical conductivity of the saturated paste extract ( $\text{EC}_e$ ), we followed the procedure proposed by [23]:

$$\text{EC}_e = \left( 1.054 + \frac{283.4}{49.699 + 0.524 \times \text{Clay}\% - 0.339 \times \text{Sand}\%} \right) \times \text{EC}_{1:5}$$

Soil organic matter was estimated by the Walkley–Black method [24]. Available phosphorus was determined by the Bray–Kurtz I method, using a solution of 0.03 M  $\text{NH}_4\text{F}$  and 0.025 M HCl ( $\text{pH} \approx 2.6$ ) as extractant [25]. Exchangeable bases ( $\text{Ca}^{2+}$ ,  $\text{Mg}^{2+}$ ,  $\text{K}^+$ , and  $\text{Na}^+$ ) were extracted with 1 M ammonium acetate ( $\text{NH}_4\text{OAc}$ ) adjusted to  $\text{pH} 7.0$  and quantified according to [26]. Effective cation exchange capacity (ECEC) was calculated as the sum of exchangeable cations. Bulk density ( $\text{g cm}^{-3}$ ) was estimated using pedotransfer functions reported by [27,28]. In general form, the pedotransfer relationship used can be expressed as:

$$\text{BD} = 1.66 - (0.004 \times \text{Clay}) - (0.002 \times \text{Silt}) - (0.005 \times \text{OM})$$

## 2.4. Construction of the Weighted Soil Quality Index (SQIw)

In this study, soil quality was operationally defined as the soil's capacity to sustain quinoa productivity under high-Andean conditions while maintaining key physicochemical functions regulating salinity–sodicity stress, nutrient availability, organic matter dynamics, structural stability, and water retention. Accordingly, the SQIw was conceived as a function-oriented index rather than a purely statistical construct. Indicator selection followed a two-stage procedure in which variables were first screened based on expert knowledge regarding their agronomic relevance for quinoa cultivation under saline–sodic high-Andean conditions, and subsequently refined through multivariate analysis to reduce redundancy among correlated properties. Within this framework, principal component analysis was used to assign relative weights among functionally meaningful indicators

rather than to define soil quality itself. The resulting minimum data set, therefore, represents complementary soil process domains, ensuring that the SQI<sub>w</sub> preserves agronomic interpretability while maintaining statistical robustness.

#### 2.4.1. Selection of the Minimum Data Set (MDS)

Soil variables were first subjected to a preliminary statistical diagnosis by calculating skewness to assess their distributions. Variables with pronounced skewness (skewness > 1.0) were log-transformed, and those with moderate skewness ( $0.5 < \text{skewness} \leq 1.0$ ) were square-root transformed. After transformation, variables were standardised to z-scores (mean = 0, standard deviation = 1) to remove unit effects and ensure comparability across different scales.

Redundancy among variables was then assessed using a Pearson correlation matrix. Variable pairs showing high collinearity ( $|r| > 0.70$ ) were considered redundant; in each such pair, one variable was removed, preferentially retaining the variable with the stronger relationship to the target metric or greater analytical reliability. The remaining variables were submitted to principal component analysis (PCA) using the FactoMineR package. Components with eigenvalues > 1 (Kaiser criterion) were retained, and for each retained component, the two variables with the largest absolute loadings were selected to form the MDS.

Following correlation filtering and PCA, the final minimum data set (MDS) comprised organic matter (OM), exchangeable sodium (Na), effective cation exchange capacity (ECEC), clay, sand, electrical conductivity (EC), and available phosphorus (P), which were subsequently normalised using the thresholds presented in Table 1.

**Table 1.** Theoretical thresholds and response types of soil variables used for normalising the weighted soil quality index (SQI<sub>w</sub>) for quinoa cultivation.

Variable	Lmin	Lopt_low	Lopt_high	Lmax	Response Type	Reference
OM (%)	1	—	—	5	More is better	[29,30]
Na (cmol kg <sup>-1</sup> )	0	—	—	4	Less is better	[31,32]
ECEC (cmol kg <sup>-1</sup> )	10	—	—	30	More is better	[33]
Clay (%)	5	10	30	40	Optimal range	[34]
Sand (%)	20	40	60	80	Optimal range	[34]
EC (dS m <sup>-1</sup> )	2	—	—	12	Less is better	[35]
P (mg kg <sup>-1</sup> )	15	—	—	30	More is better	[36,37]

#### 2.4.2. Assignment of Weights to the MDS Variables

Principal component analysis (PCA) was applied to the MDS to calculate the relative weights ( $W_i$ ) of each variable based on their contributions to the principal components that together accounted for at least 70% of the cumulative variance. The weight assigned to each variable was obtained as a weighted sum of its individual contributions ( $C_{ij}$ ), adjusted by the proportion of variance explained by each component ( $V_j$ ), following the expression:

$$W_i = \frac{\sum_{j=1}^p (C_{ij} \times V_j)}{\sum_{j=1}^p V_j}$$

#### 2.4.3. Normalisation of Variables

The MDS variables were normalised to a dimensionless scale ranging from 0 to 1, where values approaching 1 indicate favourable soil quality conditions and values close to 0 reflect limiting conditions. Threshold values (Lmin, Lopt\_low, Lopt\_high, and Lmax) were defined based on agronomically informed criteria for quinoa cultivation

under high-Andean conditions, supported by published tolerance ranges, soil fertility interpretation guidelines, and documented crop responses (Table 1). These thresholds represent, respectively, the lower limiting value, the lower bound of the optimal interval, the upper bound of the optimal interval, and the upper limiting value.

Normalisation was performed using piecewise linear scoring functions, ensuring continuity at each threshold and direct consistency with agronomic interpretation. Depending on the expected relationship between each indicator and soil quality, three response patterns were considered. For indicators in which increasing values improve soil functionality, the normalised score was calculated as:

$$M(x) = \begin{cases} 0; & \text{if } x \leq L_{min} \\ \frac{x-L_{min}}{L_{max}-L_{min}}; & \text{if } L_{min} < x < L_{max} \\ 1; & \text{if } x \geq L_{max} \end{cases}$$

For indicators where increasing values represent degradation or restriction, the score was computed as:

$$L(x) = \begin{cases} 1; & \text{if } x \leq L_{min} \\ \frac{L_{max}-x}{L_{max}-L_{min}}; & \text{if } L_{min} < x < L_{max} \\ 0; & \text{if } x \geq L_{max} \end{cases}$$

For variables characterised by an agronomic optimal interval, a trapezoidal linear function was applied, assigning a full score within the optimal range and decreasing proportionally toward limiting conditions:

$$OR(x) = \begin{cases} 0; & \text{if } x \leq L_{min} \\ \frac{x-L_{min}}{L_{opt\_low}-L_{min}}; & \text{if } L_{min} < x < L_{opt\_low} \\ 1; & \text{if } L_{opt\_low} \leq x \leq L_{opt\_high} \\ \frac{L_{max}-x}{L_{max}-L_{opt\_high}}; & \text{if } L_{opt\_high} < x < L_{max} \\ 0; & \text{if } x \geq L_{max} \end{cases}$$

These piecewise linear functions allow gradual transitions between limiting and optimal conditions, avoiding abrupt discontinuities and ensuring proportional score variation across the entire range of measured values. This structure enhances interpretability and reduces sensitivity to minor variations in threshold definition.

#### 2.4.4. Calculation of the Weighted Soil Quality Index (SQI<sub>w</sub>)

The SQI<sub>w</sub> was calculated by linearly combining the normalised values ( $N_i$ ) of the selected indicators, weighted according to their relative contributions ( $W_i$ ) derived from the PCA. The index was computed using the following expression:

$$SQI_W = \sum_{i=1}^n (W_i \times N_i)$$

They are classified as very low (<0.3), low (0.3–0.5), moderate (0.5–0.6), high (0.6–0.7), and very high (>0.7).

#### 2.5. Estimation of Soil Nutrient Supply and Agricultural Gypsum Requirement

Potential soil phosphorus (P) contribution was estimated following the method proposed by [38], which incorporates a phosphorus availability factor (AF) based on soil pH ([39]; Table S1), an assimilation coefficient (AC) of 0.3, and a nutrient use efficiency (NUE) of 30%. Similarly, potential soil potassium (K) supply was estimated using an availability factor dependent on soil cation exchange capacity and a nutrient use efficiency of

70% ([40]; Table S2). Potential soil nitrogen (N) contribution was estimated from soil organic matter (OM), assuming that 3% of OM corresponds to structural organic nitrogen (ON), with an annual mineralisation rate of 1.5% and a nutrient use efficiency of 50% [18,41,42]. In all subsequent equations, TSW refers to total soil weight:

$$P_2O_5 = \left( \frac{TSW \times P}{1000} \right) \times AF \times AC \times 2.29$$

$$K_2O = \left( \frac{TSW \times K}{1000} \right) \times AF \times 1.2$$

$$N(\text{kg ha}^{-1}) = TSW \times \frac{\%OM}{100} \times \frac{\%ON}{100} \times \frac{Mineralization}{100} \times 1000$$

$$TSW(\text{t ha}^{-1}) = BD \times 0.20 \text{ m} \times 10,000 \text{ m}^2$$

These calculations represent potential nutrient contribution estimates derived from literature-based coefficients under comparable agroecological conditions. They do not aim to quantify exact nutrient fluxes or predict crop uptake with mechanistic precision. Rather, they provide internally consistent values to assess and compare spatial variability in nutrient provisioning capacity across the study area.

The requirement for agricultural gypsum is typically calculated as the amount of exchangeable sodium that must be neutralised with calcium at a given soil depth [43]. It was computed using the following equation:

$$GR = 0.00086 \times BD \times D \times ECEC \times (ESP_i - ESP_f)$$

where ECEC ( $\text{cmol kg}^{-1}$ ) is the effective cation exchange capacity, obtained as the sum of exchangeable bases; BD ( $\text{g cm}^{-3}$ ) is soil bulk density; D (cm) is the sampling depth;  $ESP_i$  (%) is the current exchangeable sodium percentage; and  $ESP_f$  is the target value (5%) to be achieved through gypsum application. Finally, GR is the gypsum requirement expressed in  $\text{t ha}^{-1}$ .

The calculated GR represents a theoretical stoichiometric requirement of  $\text{Ca}^{2+}$  needed to replace exchangeable Na under ideal exchange conditions. Actual field effectiveness may be influenced by additional soil chemical factors, including carbonate content, salinity levels, ionic strength, and spatial variability in ECEC, which can affect gypsum dissolution,  $\text{Ca}^{2+}$  activity, and exchange reactions. Therefore, GR values should be interpreted as baseline amendment estimates for comparative and diagnostic purposes rather than exact field application prescriptions.

## 2.6. Comparative Analysis of Gypsum Requirement and Soil N, P, and K Supply Across SQIw Classes

Differences in gypsum amendment requirement and primary macronutrient supply across soil quality classes were assessed using non-parametric tests. A Kruskal–Wallis test was applied to detect overall effects ( $p < 0.05$ ), followed by pairwise Dunn's tests with Bonferroni adjustment.

Although the Kruskal–Wallis test assumes independence among observations, spatial dependence was explicitly addressed in the geostatistical modelling stage; therefore, the comparative analysis should be interpreted within this context.

## 2.7. Regression Kriging

Regression–kriging (RK) was applied for the spatial prediction of SQIw by integrating a deterministic regression component with the spatial interpolation of residuals. The environ-

mental covariates used as predictors are listed in Table 2 and include topographic variables, topographic indices, landform classes, vegetation indices, and climatic variables.

**Table 2.** Environmental predictors.

Variable	Description
Topographic variables	Digital Elevation Model (DEM); slope; aspect; hillshade
Topographic indices	Topographic Position Index (TPI); Terrain Ruggedness Index (TRI); Topographic Wetness Index (TWI)
Landform classification	Geomorphons (categorical variable with 10 landform classes: flat, summit, ridge, shoulder, spur, slope, hollow, footslope, valley, and depression)
Vegetation indices	Normalised Difference Vegetation Index (NDVI); Soil-Adjusted Vegetation Index (SAVI); Normalised Difference Water Index (NDWI)
Climatic variables	Annual total precipitation; annual mean temperature

First, a multiple linear regression model was fitted between SQI<sub>w</sub> and the selected covariates:

$$Z(S_i) = \beta_0 + \sum_{k=1}^p \beta_k X_k(S_i) + \varepsilon(S_i)$$

where  $X_k(S_i)$  represent the environmental predictors described in Table 2,  $\beta_k$  are the regression coefficients, and  $\varepsilon(S_i)$  are the residuals. Multicollinearity among predictors was evaluated using the variance inflation factor (VIF), and only variables with VIF < 5 were retained.

The residuals were subsequently interpolated using ordinary kriging, and the final RK prediction at an unsampled location  $S_0$  was obtained as:

$$\hat{Z}(S_0) = \hat{m}(S_0) + \hat{\varepsilon}(S_0)$$

where  $\hat{m}(S_0)$  is the regression estimate and  $\hat{\varepsilon}(S_0)$  is the kriged residual obtained using ordinary kriging [44].

### 2.8. Model Validation

The semivariogram model was selected based on the fit metrics RMSE,  $R^2$ , and MAE, considering as optimal the model with the lowest RMSE and MAE values and an  $R^2$  close to 1 [45,46]. Experimental semivariograms were computed for the residuals and fitted using theoretical models. Among the tested models (spherical, exponential, and Gaussian), the spherical semivariogram model showed the best performance and was therefore selected.

Validation of the kriging interpolations was performed using the leave-one-out method [47]. The validation was conducted using 198 soil samples, and model performance was evaluated using the following statistics:

$$RMSE = \sqrt{\frac{1}{n} \sum_{i=1}^n [Z_1(x_i) - Z_2(x_i)]^2}$$

$$MAE = \frac{1}{n} \sum_{i=1}^n |Z_1(x_i) - Z_2(x_i)|$$

$$R^2 = 1 - \frac{\sum_{i=1}^n [Z_1(x_i) - Z_2(x_i)]^2}{\sum_{i=1}^n [Z_1(x_i) - \bar{Z}_1]^2}$$

where  $n$  represents the number of samples, and  $Z_1(x_i)$  and  $Z_2(x_i)$  denote the predicted and observed values at site  $i$ , respectively.

### 3. Results

#### 3.1. Statistical Distribution of Soil Properties in the Agricultural Soils of the Cabana District

Soils in the Cabana district exhibited substantial physicochemical heterogeneity. pH ranged from strongly acidic to moderately alkaline (mean  $6.61 \pm 0.94$ ), while electrical conductivity showed extreme variability ( $3.30 \pm 4.87$  dS m<sup>-1</sup>; CV = 147%), indicating conditions from non-saline to highly saline. Organic matter content ( $2.61 \pm 1.93\%$ ; CV = 74%) suggested intermediate but spatially uneven fertility. Available P ( $36.13 \pm 47.78$  mg kg<sup>-1</sup>) and K ( $390.82 \pm 329.13$  mg kg<sup>-1</sup>) displayed broad ranges (CV > 80%), reflecting zones of deficiency alongside areas of nutrient accumulation driven by contrasting fertiliser management. Exchangeable Ca, Mg, K, and Na also showed high dispersion (CV = 71–118%), with effective CEC ( $22.17$  cmol kg<sup>-1</sup>) indicating medium-to-high fertility, but localised alkalinisation ( $\text{CaCO}_3 = 2.40\%$ , CV = 221%) pointed to sodicity and secondary carbonate precipitation. Textures ranged from loam to silt loam, suitable for quinoa cultivation. Overall, the soils exhibited pronounced spatial variability linked to topography, texture, and management, underscoring the need for spatially explicit soil quality assessment and site-specific management strategies (Table 3).

**Table 3.** Descriptive statistics for 14 physicochemical parameters related to the potential and current fertility of quinoa-cultivated soils.

Variable	Unidad	Mean	SD	CV	Min	Median	Max
pH	unit	6.61	0.94	14.16	4.50	6.40	8.70
EC	dS m <sup>-1</sup>	3.30	4.87	147.37	0.21	1.55	34.37
OM	%	2.61	1.93	74.08	0.50	2.10	9.50
P	mg Kg <sup>-1</sup>	36.13	47.78	132.26	0.20	19.60	342.30
K	mg Kg <sup>-1</sup>	390.82	329.13	84.21	12.00	312.80	3049.80
Sand	%	43.63	15.48	35.49	7.95	42.31	81.88
Silt	%	39.42	13.58	34.45	8.16	39.44	81.79
Clay	%	16.94	7.50	44.25	3.47	16.08	44.39
Ca	cmol Kg <sup>-1</sup>	13.72	16.20	118.08	2.46	8.94	175.20
Mg	cmol Kg <sup>-1</sup>	3.65	3.10	84.96	0.29	2.60	21.00
Kexc	cmol Kg <sup>-1</sup>	1.00	0.84	84.25	0.03	0.80	7.80
Na	cmol Kg <sup>-1</sup>	3.79	2.73	71.92	0.40	3.49	22.60
ECEC	cmol Kg <sup>-1</sup>	22.17	17.65	79.63	6.72	17.55	183.40
CaCO <sub>3</sub>	%	2.40	5.29	220.86	0.00	0.00	37.80

#### 3.2. Multivariate Statistical Analysis for Selection of the Minimum Data Set (MDS)

The correlation matrix (Figure 3) revealed significant associations among several physicochemical soil properties, indicating potential redundancy within the data set. Strong positive correlations were observed between pH and CaCO<sub>3</sub> ( $r = 0.86$ ), between ECEC and exchangeable Ca ( $r = 0.91$ ), and between sand content and bulk density ( $r = 0.95$ ). A strong negative correlation was also detected between sand and silt percentages ( $r = -0.87$ ), reflecting the compositional dependence among soil texture fractions.

To ensure that the minimum data set (MDS) represented independent soil functions rather than duplicated information, variable exclusion was based not only on correlation magnitude ( $|r| > 0.70$ ) but also on functional representativeness and agronomic relevance for quinoa production under high-Andean conditions.

Calcium carbonate (CaCO<sub>3</sub>) was excluded because its influence in these soils is primarily expressed through soil alkalinity. Given its strong association with pH, retaining both variables would have overrepresented carbonate-driven chemical processes without providing additional independent information. Soil reaction (pH) was considered the more integrative and agronomically interpretable indicator of nutrient availability constraints.

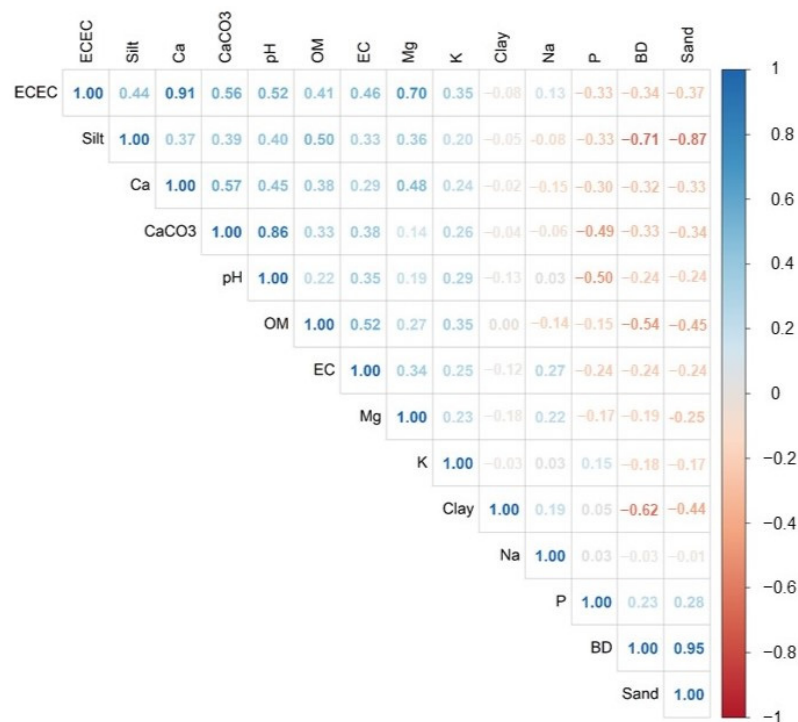


**Figure 3.** Pearson bivariate correlation matrix among 14 physicochemical soil variables. Only statistically significant correlations are shown ( $p < 0.001$ ).

Exchangeable Ca was removed due to its very high correlation with ECEC. Since ECEC represents the total pool of exchangeable bases and reflects overall charge balance and nutrient-retention capacity, it provides a more comprehensive descriptor of soil chemical fertility than Ca alone. Retaining Ca in addition to ECEC would have disproportionately weighted calcium-dominated exchange processes.

Silt was excluded because of its strong inverse relationship with sand and the inherent mathematical dependency among texture fractions. Sand and clay were retained because they better capture the functional extremes of the textural gradient relevant to quinoa performance, namely drainage, aeration, water, and nutrient retention. Including silt would have introduced compositional redundancy without enhancing functional interpretation.

Bulk density was excluded due to its near-perfect correlation with sand content. In the studied soils, bulk density variability is largely texture-driven rather than associated with independent compaction or structural degradation processes. Sand was retained as the primary physical indicator because it directly reflects particle size distribution and is less affected by estimation uncertainty derived from pedotransfer functions. Including both variables would have duplicated the physical constraint signal within the index.

This selection procedure ensured that the final MDS captured distinct and complementary soil functions, salinity, sodicity, nutrient supply, organic matter dynamics, texture, and charge balance, thereby improving the robustness and interpretability of the SQIw.

The PCA identified four principal components (PCs) with eigenvalues  $> 1$ , together explaining 72.26% of the total variance (Table 4). PC1 accounted for 33.05% of the variance and showed strong associations with ECEC (0.847), EC (0.698), pH (0.659), OM (0.656), and Mg (0.655), representing a gradient of chemical fertility and cation exchange capacity. PC2 (14.32%) was defined by a strong negative loading for clay ( $-0.930$ ) and a positive loading for sand (0.650), characterising soil texture and structural conditions. PC3 (12.88%) was dominated by P (0.718) and Na (0.518), reflecting a component associated with phosphorus availability and sodicity risk. PC4 (12.01%) highlighted the influence of Na (0.732) and OM ( $-0.501$ ), representing an axis linked to sodicity and organic matter dynamics.

**Table 4.** Principal component analysis (PCA) of soil physicochemical variables.

PCs <sup>a</sup>	PC1	PC2	PC3	PC4
Eigenvalue	3.304	1.431	1.288	1.201
Variance (%)	33.046	14.318	12.882	12.01
Cumulative Variance (%)	33.046	47.364	60.247	72.257
Factor loadings/eigen vector for each variable <sup>b,c</sup>				
pH	<b>0.659</b>	0.138	−0.378	0.086
EC	<b>0.698</b>	0.097	0.173	0.075
OM	<b>0.656</b>	−0.125	0.037	<b>−0.501</b>
P	−0.468	−0.037	<b>0.718</b>	−0.326
Kav	0.468	0.040	0.454	−0.458
Mg	<b>0.655</b>	0.220	0.293	0.229
Na	0.156	−0.180	<b>0.518</b>	<b>0.732</b>
Sand	<b>−0.585</b>	<b>0.650</b>	0.178	0.117
Clay	−0.048	<b>−0.930</b>	0.052	0.089
ECEC	<b>0.847</b>	0.126	0.073	0.106

<sup>a</sup> Only components with eigenvalues > 1 (Kaiser criterion) and cumulative variance ≥ 70% are presented.

<sup>b</sup> Variables in bold have absolute loadings ≥ 0.50. <sup>c</sup> Variables with underlined factor loadings are considered highly weighted and were selected for the MDS.

Based on the highest absolute loadings within each component, the variables selected for the minimum data set (MDS) were EC, OM, available P, exchangeable Na, sand, clay, and ECEC. These indicators capture the principal dimensions of soil variability and form the core set for calculating the weighted soil quality index (SQIw).

### 3.3. Edaphic Influence of the MDS Variables on the Weighted Soil Quality Index (SQIw)

The weighting values ( $W_i$ ) derived for the MDS variables (Figure 4) reflect their relative contribution to the weighted soil quality index (SQIw). Exchangeable sodium (Na) and available phosphorus (P) showed the highest weights ( $W_i = 0.160$  and  $0.158$ ), indicating their dominant influence on soil quality across quinoa-growing areas. In contrast, electrical conductivity (EC) and effective cation exchange capacity (ECEC) exhibited the lowest weights ( $0.135$  and  $0.107$ ), suggesting more limited spatial variability despite their continued relevance to soil chemical fertility. Overall, these patterns highlight the central role of sodicity and phosphorus availability, followed by texture and organic matter, in shaping the edaphic conditions that govern soil aeration, moisture retention, and nutrient supply.

The SQIw frequency distribution (Figure 5) exhibited an approximately normal pattern, with values ranging from 0.22 to 0.84, indicating intermediate edaphic variability across the study area. Based on the established classification thresholds, SQIw values were grouped into five soil quality classes: very low (<0.30), low (0.30–0.50), moderate (0.50–0.60), high (0.60–0.70), and very high (>0.70). The moderate class accounted for the largest proportion of observations (31.8%), followed by the high (29.2%) and low (27.3%) classes. In contrast, the very high and very low classes represented only 9.9% and 1.9% of the samples, respectively. This distribution highlights the predominance of intermediate soil quality conditions, with relatively few sites exhibiting extreme values, suggesting a moderate degree of homogeneity in the productive capacity of the assessed soils.

The mean values ( $\pm$ SD) of the MDS variables across SQIw classes (Table 5) reveal patterns consistent with the interpretation of the weighted soil quality index. Soils classified as very high and high quality exhibited greater concentrations of organic matter ( $4.17 \pm 1.63\%$  and  $3.16 \pm 2.40\%$ ) and available phosphorus ( $81.65 \pm 83.50$  and  $45.96 \pm 42.54 \text{ mg kg}^{-1}$ ), together with lower levels of exchangeable sodium ( $2.43 \pm 1.98$  and  $3.16 \pm 1.50 \text{ cmol kg}^{-1}$ ) and electrical conductivity ( $2.82 \pm 4.00$  and  $2.33 \pm 2.93 \text{ dS m}^{-1}$ ). These conditions reflect more balanced soil chemistry and a more favourable environment for plant development.

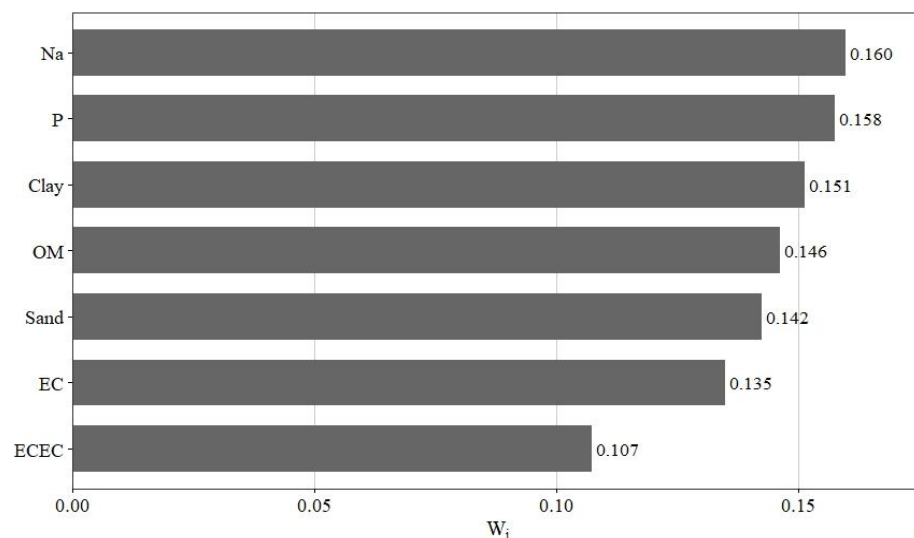


**Figure 4.** Relative weights ( $W_i$ ) of the minimum data set (MDS) indicators used to compute the weighted soil quality index (SQI<sub>w</sub>).

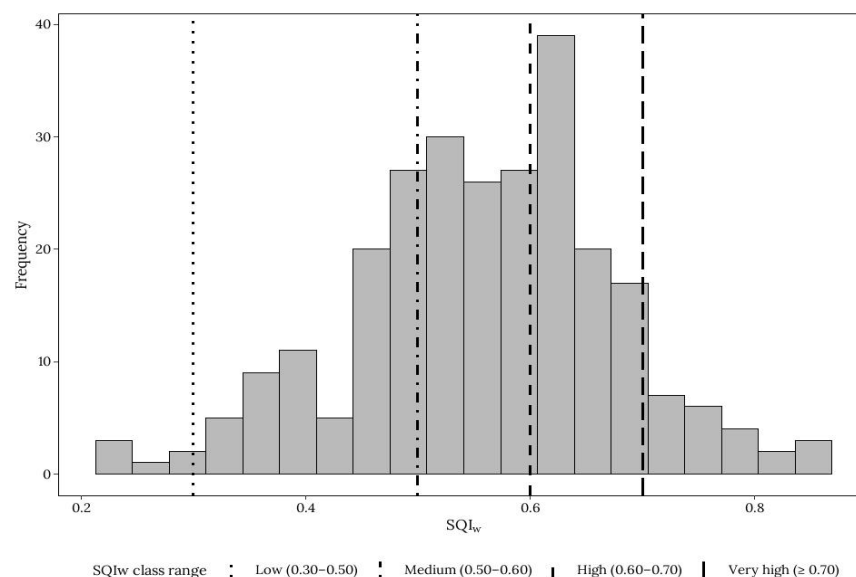


**Figure 5.** Distribution of the weighted soil quality index (SQI<sub>w</sub>) in quinoa-cultivated soils of the Cabana district, Puno.

**Table 5.** Mean values of the soil variables across different SQI<sub>w</sub> classes.

Variable	Pearson Correlation	SQI <sub>w</sub>				
		Very High	High	Medium	Low	Very Low
Na (cmol kg <sup>-1</sup> )	−0.44	2.43 ± 1.98	3.16 ± 1.50	3.56 ± 1.43	4.79 ± 3.64	10.29 ± 7.26
OM (%)	0.31	4.17 ± 1.63	3.16 ± 2.40	2.09 ± 1.37	2.09 ± 1.63	2.12 ± 0.98
ECEC (cmol kg <sup>-1</sup> )	−0.02	20.24 ± 6.34	23.64 ± 20.41	21.53 ± 20.29	21.52 ± 14.12	29.65 ± 9.65
Clay (%)	0.03	16.72 ± 5.24	16.36 ± 6.99	18.01 ± 6.92	15.84 ± 7.93	25.00 ± 18.79
Sand (%)	0.06	41.61 ± 9.53	44.04 ± 11.40	44.90 ± 15.85	43.90 ± 19.65	22.59 ± 6.31
EC (dS m <sup>-1</sup> )	−0.20	2.82 ± 4.00	2.33 ± 2.93	2.28 ± 3.28	5.40 ± 7.11	7.69 ± 5.21
P (mg kg <sup>-1</sup> )	0.48	81.65 ± 83.50	45.96 ± 42.54	32.58 ± 43.90	15.29 ± 20.82	7.54 ± 3.37
pH	−0.17	6.63 ± 0.89	6.53 ± 0.84	6.46 ± 0.88	6.82 ± 1.07	7.52 ± 0.54
K (mg kg <sup>-1</sup> )	0.20	565.34 ± 318.98	418.46 ± 391.71	354.97 ± 292.31	335.43 ± 284.72	457.68 ± 242.26
Ca (cmol kg <sup>-1</sup> )	0.16	12.77 ± 4.83	15.81 ± 19.22	13.96 ± 19.58	11.81 ± 10.52	9.99 ± 2.85
Mg (cmol kg <sup>-1</sup> )	−0.11	3.59 ± 3.01	3.61 ± 2.80	3.09 ± 1.95	4.06 ± 4.01	8.20 ± 5.19
Silt (%)	−0.06	41.67 ± 7.67	39.60 ± 10.42	37.09 ± 12.12	40.26 ± 18.30	52.42 ± 18.38

Table 5. Cont.

Variable	Pearson Correlation	SQIw				
		Very High	High	Medium	Low	Very Low
CaCO <sub>3</sub> (%)	−0.12	2.98 ± 4.88	3.32 ± 8.19	1.34 ± 2.38	2.40 ± 3.80	2.80 ± 1.29
BD (g cm <sup>−3</sup> )	−0.02	1.49 ± 0.03	1.50 ± 0.04	1.50 ± 0.05	1.51 ± 0.05	1.44 ± 0.04
ESP (%)	−0.40	12.23 ± 7.72	17.87 ± 9.52	20.87 ± 8.88	25.05 ± 13.12	31.77 ± 18.56

In contrast, very low-quality soils showed the highest sodicity ( $10.29 \pm 7.26 \text{ cmol kg}^{-1}$ ) and salinity ( $7.69 \pm 5.21 \text{ dS m}^{-1}$ ), combined with low phosphorus availability ( $7.54 \pm 3.37 \text{ mg kg}^{-1}$ ) and reduced organic matter content ( $2.12 \pm 0.98\%$ ). These characteristics denote chemically restrictive conditions that limit both soil fertility and structural stability.

Textural differences among SQIw classes were also evident: higher-quality soils tended to exhibit more balanced textures, whereas lower-quality soils showed reduced sand content and increased clay proportions.

### 3.4. Non-Parametric Comparison of Agricultural Gypsum Requirement and Soil N, P, and K Supply Across SQIw Classes in the Cabana District, Puno

The non-parametric analysis showed clear and significant differences in agricultural gypsum requirement (GR) and macronutrient supply across soil quality classes (Figure 6). High- and very high-quality soils required the least gypsum and supplied the highest amounts of N and P, whereas moderate-, low-, and very low-quality soils exhibited progressively higher GR and reduced nutrient contributions. This behaviour reflects an inverse relationship between soil quality and sodicity, whereby more fertile soils—characterised by higher organic matter and more stable physicochemical conditions—provide a greater nutrient-supplying capacity.

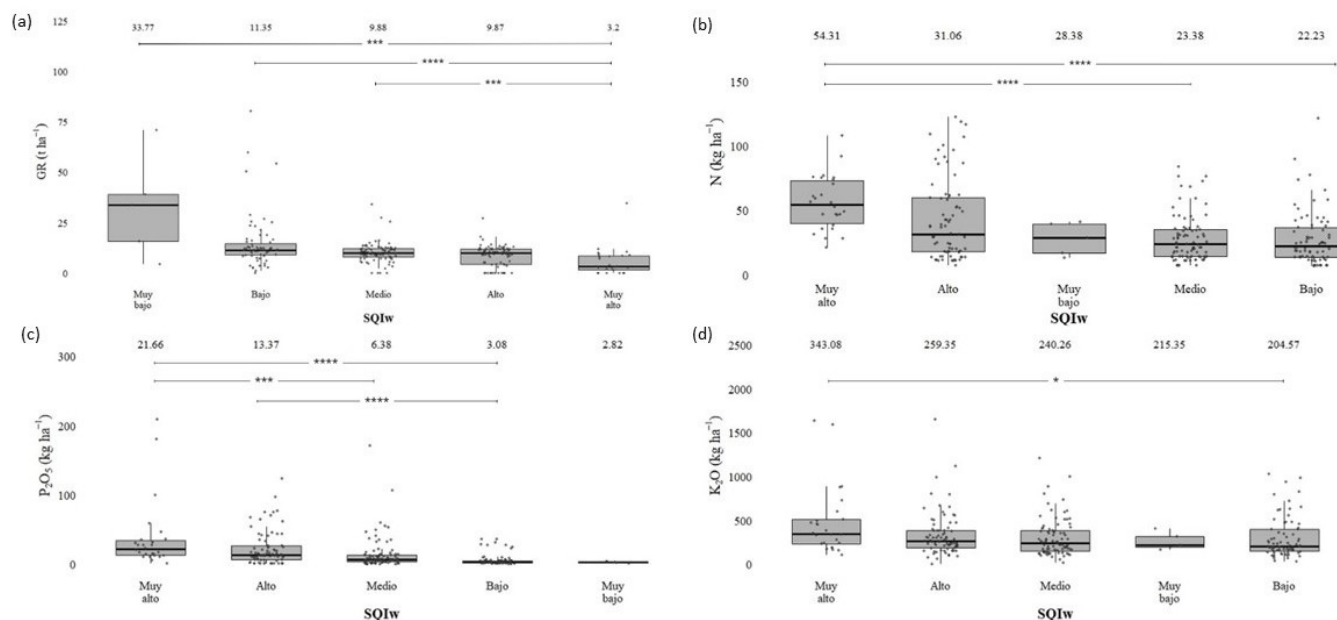


Figure 6. Comparison of (a) agricultural gypsum requirement (GR) and (b) soil-supplied nitrogen (N), (c) phosphorus (P<sub>2</sub>O<sub>5</sub>), and (d) potassium (K<sub>2</sub>O) across SQIw soil quality classes in the Cabana district, Puno. Significance levels are based on Dunn’s post hoc test following a Kruskal–Wallis analysis, with Bonferroni correction for multiple comparisons. Statistical significance is denoted as \*\*\*\*  $p < 0.0001$ , \*\*\*  $p < 0.001$ , and \*  $p < 0.05$ .

Phosphorus displayed the strongest gradient across classes, decreasing steadily toward lower SQIw levels. Potassium showed minor variation, with significant differences only

between the very high and low classes, and remained high across all categories, indicating that K is not a limiting factor for quinoa production.

Overall, declining soil quality is associated with deteriorating chemical fertility (particularly N and P depletion) and increased gypsum requirement. These patterns confirm the robustness of SQIw as an integrative indicator of soil functional status and its value for guiding site-specific and sustainable soil management in Cabana's agricultural systems.

### 3.5. Spatial Modelling and Zonation of the Soil Quality Index (SQIw)

A regression-kriging model was applied in the Cabana district to generate a continuous map of the weighted soil quality index (SQIw). Thirteen environmental predictors were used: the deterministic trend was first modelled through multiple regression, followed by ordinary kriging of the residuals to capture remaining spatial dependence. Table 6 reports the cross-validation metrics for SQIw, P<sub>2</sub>O<sub>5</sub>, N, K<sub>2</sub>O, and agricultural gypsum requirement (GR). The model indicates a moderate predictive performance, with SQIw showing the highest explanatory capacity ( $R^2 = 0.56$ ) and the lowest prediction errors (RMSE = 0.05; MAE = 0.04). Similar moderate performances were observed for P<sub>2</sub>O<sub>5</sub> ( $R^2 = 0.54$ ), N ( $R^2 = 0.50$ ), K<sub>2</sub>O ( $R^2 = 0.39$ ), and gypsum requirement ( $R^2 = 0.49$ ).

**Table 6.** Cross-validation statistics for the prediction models of gypsum requirement, soil nutrient supply, and the weighted soil quality index (SQIw).

Model	RMSE	MAE	R <sup>2</sup>
GR	2.19	1.40	0.49
P <sub>2</sub> O <sub>5</sub>	22.74	14.41	0.54
N	8.07	5.73	0.50
K <sub>2</sub> O	158.87	105.98	0.39
SQIw	0.05	0.04	0.56

Accordingly, the generated maps depict relative spatial patterns and gradients of SQIw and nutrient-related variables across the district, supporting regional-scale zonation and comparison of management units.

The total agricultural area of the Cabana district covers 15,797.37 ha. Soils with moderate fertility dominate the landscape, encompassing 85.21% of the agricultural area (13,461.19 ha), followed by high-fertility soils with 9.61% (1518 ha), and low-fertility soils representing 5.17% (817.23 ha). The spatial distribution of soil fertility is shown in Figure 7, using the following SQIw classification thresholds: low (0.30–0.50), moderate (0.50–0.60), high (0.60–0.70).

Table 7 reveals contrasting spatial patterns in the agricultural gypsum requirement (GR) and the potential supply of N, P<sub>2</sub>O<sub>5</sub>, and K<sub>2</sub>O across soils in the Cabana district. The majority of the agricultural area (12,175.65 ha; 77% of the total) falls within an intermediate GR class (9.73–14.33 t ha<sup>-1</sup>), indicating that moderate sodicity is the predominant edaphic constraint. Zones with very low (<5.14 t ha<sup>-1</sup>) or very high (18.93–23.52 t ha<sup>-1</sup>) gypsum requirements occupy only marginal areas, which indicates that extreme sodicity conditions are spatially limited.

**Table 7.** Spatial distribution of (a) agricultural gypsum requirement and potential nutrient supply of (b) N, (c) P<sub>2</sub>O<sub>5</sub>, and (d) K<sub>2</sub>O in soils of the Cabana district, Puno, Peru.

(a)	GR (t ha <sup>-1</sup> )	Total (ha)	(b)	N (kg ha <sup>-1</sup> )	Total (ha)
	<5.14	2.17		<9.55	4.40
	5.14–9.73	2717.64		9.55–29.06	8325.68

Table 7. Cont.

(a)	GR (t ha <sup>-1</sup> )	Total (ha)	(b)	N (kg ha <sup>-1</sup> )	Total (ha)
	9.73–14.33	12,175.65		29.06–48.55	6805.96
	14.33–18.93	891.25		48.55–68.05	483.20
	18.93–23.52	10.67		68.05–87.54	178.13
	Total (ha)	15,797.37		Total (ha)	15,797.37
(c)	P <sub>2</sub> O <sub>5</sub> (kg ha <sup>-1</sup> )	Total (ha)	(d)	K <sub>2</sub> O (kg ha <sup>-1</sup> )	Total (ha)
	<2.36	1.27		<84.82	0.48
	2.36–63.56	12,699.72		84.82–327.50	6392.19
	63.56–124.76	3029.82		327.50–570.17	8008.16
	124.76–185.95	62.72		570.17–812.85	1389.03
	185.95–247.15	3.84		812.85–1055.52	7.52
	Total (ha)	15,797.37		Total (ha)	15,797.37

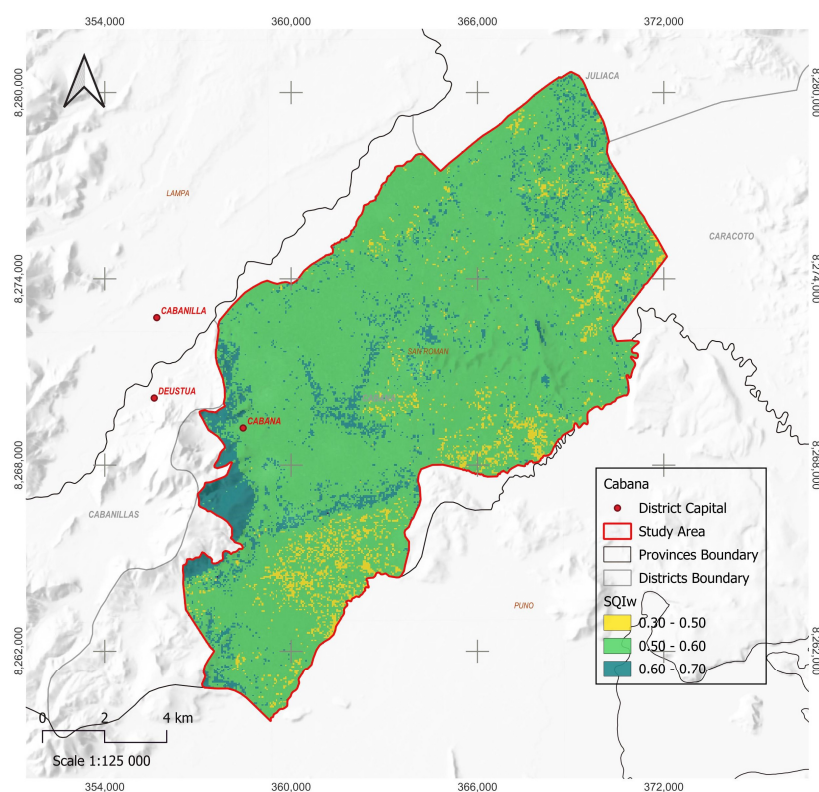


Figure 7. Spatial variability map of soil quality (SQIw) in the Cabana district, Puno.

Potential nitrogen supply exhibits a relatively homogeneous distribution but is dominated by low-to-moderate classes. The combined area of the 9.55–29.06 kg ha<sup>-1</sup> and 29.06–48.55 kg ha<sup>-1</sup> classes exceeds 15,000 ha, implying generally limited native N availability and the need for spatially variable N fertilisation strategies. Phosphorus availability is markedly skewed toward low and moderate values: the 2.36–63.56 kg ha<sup>-1</sup> class alone covers 12,699.72 ha, while higher P<sub>2</sub>O<sub>5</sub> classes occupy substantially smaller extents. This pattern identifies phosphorus as the most limiting and spatially heterogeneous nutrient, likely reflecting P fixation processes related to soil pH and carbonate content.

In contrast, potassium is widely available throughout most of the district. Substantial areas are contained within moderate-to-high K<sub>2</sub>O classes, with 8008.16 ha in the 327.50–570.17 kg ha<sup>-1</sup> range and 6392.19 ha in the 84.82–327.50 kg ha<sup>-1</sup> range, indicating

high K stability in the mineral fraction and low susceptibility to leaching. Consequently, K does not appear to limit quinoa productivity in the study area.

Collectively, the results reported in Table 7 indicate that soil fertility in Cabana is primarily constrained by sodicity and by the availability of nitrogen and phosphorus, whereas potassium is generally adequate. These spatial patterns underscore the need for differentiated soil management: prioritise gypsum amendments to ameliorate sodicity and site-specific N and P fertilisation to address nutrient deficits, thereby optimising the sustainable production of quinoa (Figure 8).

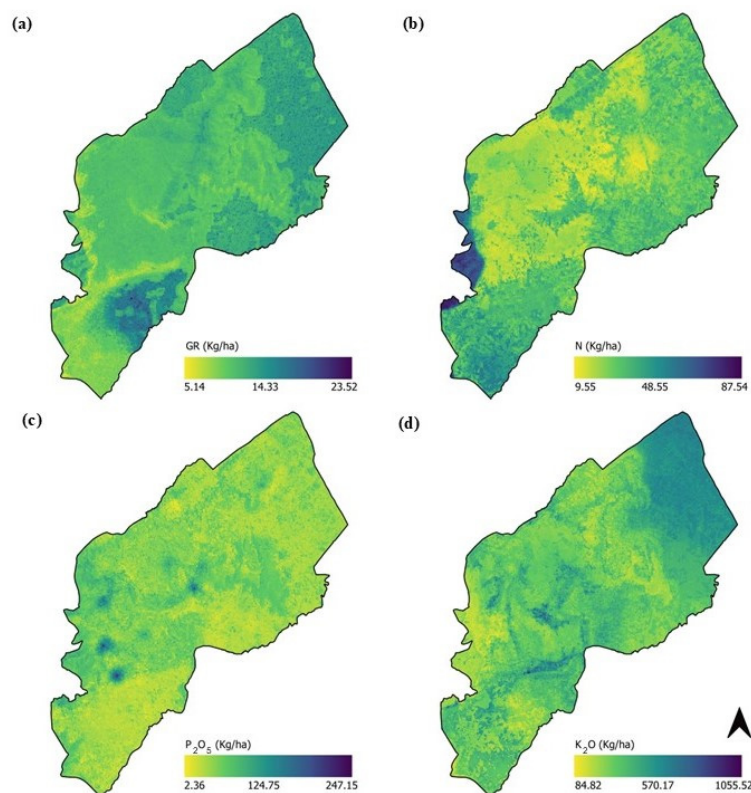


**Figure 8.** Maps showing the spatial variation of (a) agricultural gypsum requirement and the potential nutrient supply of (b) N, (c)  $P_2O_5$ , and (d)  $K_2O$  in soils of the Cabana district, Puno, Peru.

## 4. Discussions

### 4.1. Edaphic Heterogeneity in the Cabana District and Potential Constraints for Quinoa

The soil analysis in the Cabana district (Table 3) demonstrates marked spatial heterogeneity in soil properties, with particularly high coefficients of variation for key indicators such as electrical conductivity (CV = 147.4%) and available phosphorus (CV = 132.3%). This variability reflects a complex interplay between natural drivers—including topographic variability, heterogeneous geology, and a predominance of Mollisols and Cambisols—and anthropogenic pressures from non-standardised agricultural practices, such as uneven fertiliser application, likely use of saline irrigation water, and stubble burning. Despite these adverse and contrasting conditions, quinoa (*Chenopodium quinoa* Willd.) remains the dominant crop, underscoring its notable ecological plasticity. As an Andean native, quinoa has evolved in extreme environments and exhibits exceptional tolerance to a wide pH range (4.5–9.5), moderate-to-high salinity, and low-fertility soils [48,49]. In Cabana—where soils vary from strongly acidic (pH = 4.5) to moderately alkaline (pH = 8.7)—quinoa sustains acceptable growth, although yields are constrained in areas affected by extreme sodicity ( $Na^+ > 6 \text{ cmol kg}^{-1}$ ) or severe salinity ( $EC > 8 \text{ dS m}^{-1}$ ), which reduce germination, root development, and grain filling [50].

The predominantly silty-loam texture (sand 43.6%, clay 16.9%) favours drainage and aeration—attributes critical for a species that, while drought-tolerant, is sensitive to waterlogging and root hypoxia. Such conditions inhibit quinoa development in soils with high clay content and poor structure [51]. Mean soil organic matter (2.61%) improves the soil's capacity to retain moisture and nutrients, thereby influencing productive potential, particularly under the prevailing climatic regime of very low precipitation (28 mm yr<sup>-1</sup>) and high evaporative demand. Quinoa partially offsets these limitations through high water-use efficiency and the development of extensive root systems that explore larger soil volumes for resources [52].

The extreme variability of available phosphorus—ranging from acute deficiencies (<10 mg kg<sup>-1</sup>) to excessive accumulations (>300 mg kg<sup>-1</sup>)—indicates imbalanced nutrient management. Under such conditions, quinoa can survive on poor soils but fails to reach its yield potential; conversely, in nutrient-rich areas, no further yield response is evident, suggesting inefficiencies in input use. High exchangeable sodium (up to 22.6 cmol kg<sup>-1</sup> in some zones) and extreme electrical conductivity (34.37 dS m<sup>-1</sup>) further challenge quinoa's physiological tolerance. The species deploys mechanisms such as osmotic regulation, selective ion accumulation, and synthesis of protective metabolites to maintain vital functions under moderate salinity [48], but these mechanisms become overwhelmed under extreme conditions, accounting for the low productivity observed in soils classified as “very low” by the SQIw index.

Consequently, quinoa functions effectively as a biological indicator of soil quality: its widespread occurrence attests to resilience, yet its highly variable yield (1.07–1.09 t ha<sup>-1</sup> versus a potential >5 t ha<sup>-1</sup>) exposes the underlying edaphic constraints [12,13]. Although quinoa can adapt to a broad spectrum of soil conditions in the southern Altiplano, sustainable productivity will require targeted interventions to correct chemical imbalances—especially sodicity, salinity, and phosphorus deficiency—and to increase soil organic matter through agroecological practices. Recognising this duality—high tolerance but limited productive response in degraded soils—is essential to devise management strategies that exploit quinoa's robustness without accepting soil degradation as an inevitable outcome of cultivation.

#### *4.2. Interpretation of the SQIw and Its Relationship with Soil Fertility and Sodicity in High-Andean Quinoa Agroecosystems*

The soil quality index (SQIw) enabled integration of multiple physicochemical attributes into a single, highly sensitive metric for diagnosing fertility in saline-sodic soils cultivated with quinoa in the Cabana district, Puno. Significant correlations were detected between SQIw and available P ( $r = 0.48$ ), Na ( $r = -0.44$ ), exchangeable sodium percentage (ESP;  $r = -0.40$ ), organic matter (OM;  $r = 0.31$ ), electrical conductivity (EC;  $r = -0.20$ ), and available K ( $r = 0.20$ ). These results are consistent with [53], who report the superiority of integrated soil quality indices over univariate approaches, and they underscore the importance of soil quality for sustainable fertiliser management [15].

Soils classified as high and very high quality encompass approximately 1519 ha and exhibit available phosphorus concentrations of  $45.96 \pm 42.54$  mg kg<sup>-1</sup> and  $81.65 \pm 83.50$  mg kg<sup>-1</sup>, respectively. Phosphorus was among the most variable parameters (coefficient of variation = 132.36%) and showed a negative correlation with pH ( $r = -0.50$ ). Consequently, the mean pH values observed in these soils ( $6.53 \pm 0.84$  and  $6.63 \pm 0.89$ ) are compatible with conditions favourable for high P availability [54]. These differences translate into a significantly greater potential P<sub>2</sub>O<sub>5</sub> supply in high and very high-quality soils compared with low-quality soils ( $p < 0.0001$ ). Over 50% of high and very high-quality soils provide 13.37 and 21.66 kg ha<sup>-1</sup> P<sub>2</sub>O<sub>5</sub>, respectively, suggesting reduced fertiliser requirements to satisfy quinoa's P demand (60 kg ha<sup>-1</sup> P<sub>2</sub>O<sub>5</sub>) [55].

These same soils exhibited the highest organic matter contents, ranging from  $3.16 \pm 2.40\%$  to  $4.17 \pm 1.63\%$ . Organic matter is a key determinant of plant nutrition, soil physical structure, water retention, and salinity control [56]. The potential N supply was also significantly greater in very high-quality soils (median =  $54.31 \text{ kg ha}^{-1} \text{ N}$ ) compared with medium- and low-quality soils ( $23.38$  and  $22.23 \text{ kg ha}^{-1} \text{ N}$ , respectively;  $p = 0.0001$ ). These findings support site-specific fertiliser management to meet quinoa's N requirement ( $40 \text{ kg ha}^{-1}$ ) [55]. Spatial modelling of N supply identified  $661.33 \text{ ha}$  with N levels exceeding quinoa's requirement, a result that concurs with [34], who reported yields up to  $1 \text{ t ha}^{-1}$  on the Altiplano in the absence of N fertilisation.

Among the factors conditioning greater organic matter accumulation, the silt fraction was the most influential ( $r = 0.50$ ), consistent with the protective role of fine fractions in stabilising soil organic carbon [57]. Although silt percentage increases slightly between medium- and very high-quality classes, very low-quality soils displayed the highest silt contents ( $52.42 \pm 18.38\%$ ), a pattern associated with elevated salt accumulation due to limited leaching within the profile.

Conversely, soils classified from medium- to very low-quality exhibited greater sodicity concomitant with progressive declines in N and P. This is attributable to the Na/Ca imbalance characteristic of saline-sodic soils, which impairs fertility through reduced microbial activity, lower mineralisation rates, and physical soil constraints [58]. In particular, Na accumulation in quinoa grain negatively affects its nutritional quality, and sodicity has been reported to pose a greater risk than salinity [31]. The dominant textural classes were loam to silty-loam; [59] indicate that silty and clayey soils are most susceptible to dispersion under elevated Na. The naturally low fertility of these soils, coupled with the prevailing high-Andean environmental conditions, directly restricts N and P availability.

One remediation option is the application of amendments, such as agricultural gypsum. These corrective amendments aim to reduce dissolved salts in the soil solution and exchangeable sodium [60]. Lower-quality soils typically require higher gypsum doses because  $\text{Ca}^{2+}$  in the cation exchange complex counteracts the dispersive effect of high Na concentrations and promotes aggregate formation [61]. In general, agricultural gypsum improves soil chemical status and alleviates low fertility by increasing sulphur, the Ca/Mg ratio, and microbial biomass within the 0–10 cm layer [62]. However, it should be noted that gypsum application tends to increase exchangeable K in the soil solution: in non-sodic soils, gypsum can raise exchangeable K by up to 78.7% [63]. Excessive gypsum application above recommended rates may also reduce arbuscular mycorrhizal fungal diversity and colonisation at deeper soil depths [64].

Relevant organic fertilisation alternatives include seabird guano, compost, and animal manure. Reference [65] demonstrated that the combined application of seabird guano (GI) and sheep manure (EO) significantly improves the physical properties of quinoa-cultivated soils. Several studies indicate that soil organic acids (humic and fulvic acids) influence inorganic phosphate availability in P-fertilised soils by inhibiting the formation of stable calcium phosphate phases [66].

#### 4.3. Spatial Predictability of Soil Quality and Fertility Constraints in High-Andean Landscapes

The predictive performance of the regression kriging (RK) model varied markedly depending on the soil indicator assessed, reflecting the spatial heterogeneity typical of high-Andean agroecosystems with complex topography and steep environmental gradients [67].

When applied to the soil quality index (SQI<sub>w</sub>), RK exhibited the greatest predictive capacity of all modelled variables, yielding a coefficient of determination ( $R^2$ ) of 0.56, a root mean square error (RMSE) of 0.05, and a mean absolute error (MAE) of 0.04. These metrics are considered satisfactory for spatial prediction studies that employ environmental

covariates [68]. RK's superiority relative to individual nutrient variables (N:  $R^2 = 0.50$ ;  $P_2O_5$ :  $R^2 = 0.54$ ;  $K_2O$ :  $R^2 = 0.39$ ) and to gypsum requirement ( $R^2 = 0.49$ ) is attributable to the integrative nature of the SQIw, which synthesises multiple interdependent edaphic properties. This result therefore supports the use of the SQIw to guide variable-rate application of amendments and fertilisers according to soil quality, providing better predictability than single-variable models.

The spatial distribution of SQIw shows that 85.21% of the landscape exhibits moderate fertility (13,461.19 ha), 9.61% exhibits high quality (1518.71 ha), and 5.17% exhibits low quality (817.23 ha). This pattern defines a heterogeneous fertility scenario with substantial productive potential but heightened vulnerability to inappropriate management. The observed inverse correlation between soil quality and gypsum requirement indicates that sodicity is the dominant limiting factor, consistent with studies showing how accumulation of exchangeable sodium leads to clay dispersion and loss of permeability [69]. Accordingly, the zoning derived from the model directs targeted amendment application in critical sectors, prioritising structural recovery via agricultural gypsum, which facilitates  $Ca^{2+}$ – $Na^+$  exchange on the cation exchange complex [69,70].

Differential analysis of the primary macronutrient status (N,  $P_2O_5$ , and  $K_2O$ ) revealed contrasting patterns that demand site-specific fertilisation strategies. Nitrogen was low to medium across 95.79% of the area, reflecting moderate organic matter contents and the low mineralization rates typical of high-Andean environments, where low temperature constrains microbial activity and thus the release of plant-available N [71,72]. Phosphorus emerged as the most limiting nutrient, with 80.40% of the territory at low levels—a pattern that may be explained by fixation processes associated with calcium carbonates and with iron and aluminium oxides that immobilise P [73]. By contrast, potassium showed a more favourable distribution (50.69% of the area at medium levels and 8.84% at high levels) and therefore does not constitute a limiting factor in most soils evaluated. These contrasts call for tailored interventions to raise N availability, correct P deficiencies, and implement rational K management focused on critical zones.

## 5. Conclusions

This study developed a weighted soil quality index (SQIw) for quinoa-cultivated soils of the Puno highlands by integrating physicochemical analyses, multivariate indicator selection, and regression–kriging modelling. The resulting minimum data set (EC, OM, available P, exchangeable Na, sand, clay, and ECEC) captured the main edaphic gradients associated with sodicity and nutrient dynamics.

The SQIw revealed moderate spatial variability ( $R^2 = 0.56$ ), with soil quality primarily constrained by exchangeable Na and phosphorus availability. Nitrogen and phosphorus deficiencies were prevalent in lower SQIw classes, whereas potassium was generally non-limiting under current soil conditions. Gypsum requirement increased consistently toward lower-quality soils, confirming the functional linkage between sodicity and soil degradation.

The resulting maps provide a regional-scale diagnostic framework to support soil management planning in high-Andean agroecosystems. As no yield-response or economic analyses were conducted, the findings should be interpreted as a biophysical assessment of soil constraints rather than as direct fertilisation prescriptions.

**Supplementary Materials:** The following supporting information can be downloaded at: <https://www.mdpi.com/article/10.3390/agronomy16070680/s1>; Table S1. Correction factors (FD) for phosphorus availability according to soil pH [39]. Table S2. Correction factors (FD) for potassium availability according to cation exchange capacity, CEC [40].

**Author Contributions:** Conceptualization, N.C.-C., S.M., M.C., and K.Q.; methodology, N.C.-C., S.M., A.C., K.C.-Z., E.C., and K.Q.; software, N.C.-C., S.M., R.M., E.C., and K.Q.; validation, N.C.-C., A.C., and K.Q.; formal analysis, N.C.-C., S.M., R.Q., and K.Q.; investigation, N.C.-C., S.M., R.M., M.C., E.C., and K.Q.; resources, N.C.-C., A.C., K.C.-Z., M.C., and K.Q.; data curation, N.C.-C., K.C.-Z., and K.Q.; writing—original draft, N.C.-C., R.Q., R.M., and K.Q.; writing—review and editing, N.C.-C., R.Q., and K.Q.; visualisation, N.C.-C., S.M., and K.Q.; supervision, N.C.-C., S.M., A.C., K.C.-Z., M.C., and K.Q.; project administration, N.C.-C. and K.Q.; funding acquisition, N.C.-C. and K.Q. All authors have read and agreed to the published version of the manuscript.

**Funding:** This research was funded by the Instituto Nacional de Innovación Agraria, grant number 2487112.

**Data Availability Statement:** Data are contained within the article and Supplementary Materials.

**Conflicts of Interest:** The authors declare no conflicts of interest.

## Nomenclature

SQIw	Weighted soil quality index
MDS	Minimum data set
PCA	Principal component analysis
RK	Regression-kriging
LOOCV	Leave-one-out cross-validation
OM	Soil organic matter
EC	Electrical conductivity
ECEC	Effective cation exchange capacity
P	Available phosphorus
Na	Exchangeable sodium
Wi	Weight assigned to variable $i$
Cij	Contribution of variable $i$ to principal component $j$
Vj	Variance explained by principal component $j$
Lmin	Lower limiting threshold
Lopt_low	Lower bound of optimal range
Lopt_high	Upper bound of optimal range
Lmax	Upper limiting threshold
RMSE	Root mean square error
MAE	Mean absolute error
R <sup>2</sup>	Coefficient of determination

## References

1. Food and Agriculture Organization of the United Nations (FAO). *Evaluación Final Del Proyecto “Gestión Sostenible de La Agrobiodiversidad y Recuperación de Ecosistemas Vulnerables en la Región Andina del Perú a Través del Enfoque de Sistemas Importantes del Patrimonio Agrícola Mundial”*—Codigo do Proyecto: GCP/PER/045/GFF—ID FMAM 9092; Serie de evaluaciones de proyectos; FAO: Roma, Italia, 2025. [CrossRef]
2. Huang, H.; Wang, Q.; Tan, J.; Zeng, C.; Wang, J.; Huang, J.; Hu, Y.; Wu, Q.; Wu, X.; Liu, C.; et al. Quinoa Greens as a Novel Plant Food: A Review of Its Nutritional Composition, Functional Activities, and Food Applications. *Crit. Rev. Food Sci. Nutr.* **2025**, *65*, 3665–3685. [CrossRef]
3. Maamri, K.; Zidane, O.D.; Chaabena, A.; Fiene, G.; Bazile, D. Adaptation of Some Quinoa Genotypes (*Chenopodium quinoa* Willd.), Grown in a Saharan Climate in Algeria. *Life* **2022**, *12*, 1854. [CrossRef] [PubMed]
4. INEI PUNO. *Compendio Estadístico 2023*; INEI PUNO: Puno, Peru, 2023.
5. Mobeena, S.; Thavaprakash, N.; Vaiyapuri, K.; Djanaguiraman, M.; Geethanjali, S.; Geetha, P. Influencia de Diferentes Tipos de Suelos En El Crecimiento y Rendimiento de La Quinoa (*Chenopodium quinoa* Willd.). *J. Appl. Nat. Sci.* **2023**, *15*, 365–370. [CrossRef]
6. Wieme, R.; Reganold, J.; Crowder, D.; Murphy, K.; Carpenter-Boggs, L. Productividad y Calidad Del Suelo de Los Sistemas de Cultivo de Forraje Orgánico, Quinoa y Cereales En Las Zonas Áridas Del Noroeste Del Pacífico, EE. UU. *Agric. Ecosyst. Environ.* **2020**, *293*, 106838. [CrossRef]

7. Nyéki, A.; Daróczy, B.; Kerepesi, C.; Neményi, M.; Kovács, A.J. Spatial Variability of Soil Properties and Its Effect on Maize Yields within Field—A Case Study in Hungary. *Agronomy* **2022**, *12*, 395. [CrossRef]
8. Hengl, T. *A Practical Guide to Geostatistical Mapping of Environmental Variables*; Europea: Madrid, Spain, 2007.
9. Hengl, T.; Heuvelink, G.B.M.; Rossiter, D.G. About Regression-Kriging: From Equations to Case Studies. *Comput. Geosci.* **2007**, *33*, 1301–1315. [CrossRef]
10. Keskin, H.; Grunwald, S. Regression Kriging as a Workhorse in the Digital Soil Mapper’s Toolbox. *Geoderma* **2018**, *326*, 22–41. [CrossRef]
11. Taaime, N.; Rafik, S.; El Mejahed, K.; Oukarroum, A.; Choukr-Allah, R.; Bouabid, R.; El Gharous, M. Worldwide Development of Agronomic Management Practices for Quinoa Cultivation: A Systematic Review. *Front. Agron.* **2023**, *5*, 1215441. [CrossRef]
12. Flórez-Martínez, D.H.; Rodríguez-Cortina, J.; Chavez-Oliveros, L.F.; Aguilera-Arango, G.A.; Morales-Castañeda, A. Current Trends and Prospects in Quinoa Research: An Approach for Strategic Knowledge Areas. *Food Sci. Nutr.* **2024**, *12*, 1479–1501. [CrossRef]
13. AlKhamisi, S.A.; Nadaf, S.; Al-Jabri, N.; Al-Hashmi, K.; Al-Shirawi, A.I.; Khan, R.R.; Al-Sulaimi, H.; Al-Azri, M. Productivity of Quinoa (*Chenopodium quinoa* L.) Genotypes across Different Agro-Ecological Regions of Oman. *Open Agric. J.* **2021**, *15*, 98–109. [CrossRef]
14. Doran, J.W.; Zeiss, M.R. Soil Health and Sustainability: Managing the Biotic Component of Soil Quality. *Appl. Soil Ecol.* **2000**, *15*, 3–11. [CrossRef]
15. Abdu, A.; Laekemariam, F.; Gidago, G.; Getaneh, L. Explaining the Soil Quality Using Different Assessment Techniques. *Appl. Environ. Soil Sci.* **2023**, *2023*, 6699154. [CrossRef]
16. AbdelRahman, M.A.E.; Zakarya, Y.M.; Metwaly, M.M.; Koubouris, G. Deciphering Soil Spatial Variability through Geostatistics and Interpolation Techniques. *Sustainability* **2021**, *13*, 194. [CrossRef]
17. Fick, S.E.; Hijmans, R.J. WorldClim 2: New 1-Km Spatial Resolution Climate Surfaces for Global Land Areas. *Int. J. Climatol.* **2017**, *37*, 4302–4315. [CrossRef]
18. Havlin, J.L.; Tisdale, S.L.; Nelson, W.L.; Beaton, J.D. *Soil Fertility and Fertilizers: An Introduction to Nutrient Management*, 6th ed.; Pearson Education India: Tamil Nadu, India, 2016; Volume 8.
19. ISO 11464:2006; Soil Quality—Pretreatment of Samples for Physico-Chemical Analysis. ISO: Vernier, Geneva, 2006. Available online: <https://www.iso.org/standard/37718.html> (accessed on 2 April 2025).
20. Ministry of the Environment and Natural Resources. (SEMARNAT) NORMA Oficial Mexicana NOM-021-RECNAT-2000, *Establishing Specifications for Soil Fertility, Salinity, and Classification*; Ministry of the Environment and Natural Resources: Singapore, 2002; p. 73.
21. United States Environmental Protection Agency. *Method 9045D: Soil and Waste pH, Part of Test Methods for Evaluating Solid Waste, Physical/Chemical Methods*; Soil Waste PH: Quezon City, Philippines, 2004; pp. 1–5.
22. ISO 11265:1994; Soil Quality—Determination of Specific Electrical Conductivity. ISO: Vernier, Geneva, 1994. Available online: <https://www.iso.org/es/contents/data/standard/01/92/19243.html> (accessed on 2 April 2025).
23. Kargas, G.; Londra, P.; Sotirakoglou, K. The Effect of Soil Texture on the Conversion Factor of 1:5 Soil/Water Extract Electrical Conductivity (EC1:5) to Soil Saturated Paste Extract Electrical Conductivity (ECe). *Water* **2022**, *14*, 642. [CrossRef]
24. Walkley, A.; Black, I.A. An examination of the dDegtjareff Method for determining soil organic matter, and a proposed modification of the chromic acid titration method. *Soil Sci.* **1934**, *37*, 29. [CrossRef]
25. Bray, R.H.; Kurtz, L.T. Determination of total, organic, and available forms of phosphorus in soils. *Soil Sci.* **1945**, *59*, 39. [CrossRef]
26. Thomas, G.W. Exchangeable Cations. In *Agronomy Monographs*; Page, A.L., Ed.; Wiley: Hoboken, NJ, USA, 1982; Volume 9, pp. 159–165, ISBN 978-0-89118-072-2.
27. Manrique, L.A.; Jones, C.A. Bulk Density of Soils in Relation to Soil Physical and Chemical Properties. *Soil Sci. Soc. Amer. J.* **1991**, *55*, 476–481. [CrossRef]
28. Rawls, W.J. Estimating Soil Bulk Density from Particle Size Analysis and Organic Matter Content 1. *Soil Sci.* **1983**, *135*, 123–125. [CrossRef]
29. Gonzales, V.; Huallpan, M.; Ramirez, X.; Miguel, Y.S.; Dubey, M.; Jensen, D.F.; Karlsson, M.; Crespo, C. Rhizosphere Bacteria from the Bolivian Highlands Improve Drought Tolerance in Quinoa (*Chenopodium quinoa* Willd.). *J. Appl. Microbiol.* **2024**, *135*, 1xae296. [CrossRef]
30. Taaime, N.; El Mejahed, K.; Oukarroum, A.; Choukr-Allah, R.; Pittelkow, C.; Bouabid, R.; Gharous, M.E. Residual Effects of Compost and Manure Fertilizers on Quinoa Production and Nutrient Uptake. *J. Soil Sci. Plant Nutr.* **2024**, *24*, 4338–4348. [CrossRef]
31. Abbas, G.; Amjad, M.; Saqib, M.; Murtaza, B.; Asif Naeem, M.; Shabbir, A.; Murtaza, G. Soil Sodicity Is More Detrimental than Salinity for Quinoa (*Chenopodium quinoa* Willd.): A Multivariate Comparison of Physiological, Biochemical and Nutritional Quality Attributes. *J. Agron. Crop Sci.* **2021**, *207*, 59–73. [CrossRef]

32. Sparks, D.L. The Chemistry of Saline and Sodic Soils. In *Environmental Soil Chemistry*; Elsevier: Amsterdam, The Netherlands, 2003; pp. 285–300, ISBN 978-0-12-656446-4.
33. Bünemann, E.K.; Bongiorno, G.; Bai, Z.; Creamer, R.E.; De Deyn, G.; De Goede, R.; Fleskens, L.; Geissen, V.; Kuyper, T.W.; Mäder, P.; et al. Soil Quality—A Critical Review. *Soil Biol. Biochem.* **2018**, *120*, 105–125. [[CrossRef](#)]
34. Cárdenas-Castillo, J.E.; Delatorre-Herrera, J.; Bascuñán-Godoy, L.; Rodríguez, J.P. Quinoa (*Chenopodium quinoa* Willd.) Seed Yield and Efficiency in Soils Deficient of Nitrogen in the Bolivian Altiplano: An Analytical Review. *Plants* **2021**, *10*, 2479. [[CrossRef](#)]
35. Chaganti, V.N.; Ganjgunte, G.K. Quinoa Growth and Yield Performance under Salinity Stress in Arid West Texas. *Agrosystems Geosci. Environ.* **2024**, *7*, e20493. [[CrossRef](#)]
36. Bouras, H.; Choukr-Allah, R.; Amouaouch, Y.; Bouaziz, A.; Devkota, K.P.; El Mouttaqi, A.; Bouazzama, B.; Hirich, A. How Does Quinoa (*Chenopodium quinoa* Willd.) Respond to Phosphorus Fertilization and Irrigation Water Salinity? *Plants* **2022**, *11*, 216. [[CrossRef](#)]
37. De Souza Campos, P.M.; Meier, S.; Morales, A.; Lavanderos, L.; Nahuelcura, J.; Ruiz, A.; López-García, Á.; Seguel, A. New Insights into the Phosphorus Acquisition Capacity of Chilean Lowland Quinoa Roots Grown under Low Phosphorus Availability. *Plants* **2022**, *11*, 3043. [[CrossRef](#)]
38. Quispe, K.; Hermoza, N.; Mejia, S.; Romero-Chavez, L.E.; Ottos, E.; Arce, A.; Solórzano Acosta, R. Spatial Analysis of Soil Acidity and Available Phosphorus in Coffee-Growing Areas of Pichanaqui: Implications for Liming and Site-Specific Fertilization. *Agriculture* **2025**, *15*, 1632. [[CrossRef](#)]
39. McFarland, M.L.; Haby, V.A.; Redmon, L.A.; Bade, D.H. *Managing Soil Acidity*; The Texas A&M University System: College Station, TX, USA, 2001.
40. Dobermann, A.R. Crop Potassium Nutrition—Implications for Fertilizer Recommendations. Available online: <https://digitalcommons.unl.edu/agronomyfacpub/> (accessed on 9 December 2025).
41. Raun, W.R.; Johnson, G.V. Improving Nitrogen Use Efficiency for Cereal Production. *Agron. J.* **1999**, *91*, 357–363. [[CrossRef](#)]
42. Smil, V. Nitrogen in Crop Production: An Account of Global Flows. *Glob. Biogeochem. Cycles* **1999**, *13*, 647–662. [[CrossRef](#)]
43. Oster, J.D.; Shainberg, I.; Abrol, I.P. Reclamation of Salt-Affected Soils. In *Agronomy Monographs*; Skaggs, R.W., Van Schilfgaarde, J., Eds.; American Society of Agronomy: Madison, WI, USA; Crop Science Society of America: Madison, WI, USA; Soil Science Society of America: Madison, WI, USA, 2015; pp. 659–691, ISBN 978-0-89118-230-6.
44. Esri Cómo Funciona Kriging—ArcGIS Pro | Documentación. Available online: <https://pro.arcgis.com/es/pro-app/latest/tool-reference/3d-analyst/how-kriging-works.htm> (accessed on 2 April 2025).
45. Bromberg, F.; Pérez, D.S. Spatial interpolation using machine learning in vineyards in the province of Mendoza, Argentina. In Proceedings of the 13th Argentine Symposium on Artificial Intelligence, La Plata, Argentina, 27–28 August 2012.
46. Fu, Y.; Song, J.; Guo, J.; Fu, Y.; Cai, Y. Prediction and Analysis of Sea Surface Temperature Based on LSTM-Transformer Model. *Reg. Stud. Mar. Sci.* **2024**, *78*, 103726. [[CrossRef](#)]
47. Fernández Villafañez, S. Tree-Based Regression and Classification Methods. 2022. Available online: <https://uvadoc.uva.es/handle/10324/53822> (accessed on 2 April 2025).
48. Bhargava, A.; Shukla, S.; Ohri, D. *Chenopodium quinoa*—An Indian Perspective. *Ind. Crops Prod.* **2006**, *23*, 73–87. [[CrossRef](#)]
49. Wali, A.M.; Kenawey, M.K.; Ibrahim, O.M.; El Lateef, E.M.A. Productivity of Quinoa (*Chenopodium quinoa* L.) under New Reclaimed Soil Conditions at North-Western Coast of Egypt. *Bull. Natl. Res. Cent.* **2022**, *46*, 38. [[CrossRef](#)]
50. Tovar, J.C.; Quillatupa, C.; Callen, S.T.; Castillo, S.E.; Pearson, P.; Shamin, A.; Schuhl, H.; Fahlgren, N.; Gehan, M.A. Heating Quinoa Shoots Results in Yield Loss by Inhibiting Fruit Production and Delaying Maturity. *Plant J.* **2020**, *102*, 1058–1073. [[CrossRef](#)]
51. Zurita-Silva, A.; Fuentes, F.; Zamora, P.; Jacobsen, S.-E.; Schwember, A.R. Breeding Quinoa (*Chenopodium quinoa* Willd.): Potential and Perspectives. *Mol. Breed.* **2014**, *34*, 13–30. [[CrossRef](#)]
52. Cancino-Espinoza, E.; Vázquez-Rowe, I.; Quispe, I. Organic Quinoa (*Chenopodium quinoa* L.) Production in Peru: Environmental Hotspots and Food Security Considerations Using Life Cycle Assessment. *Sci. Total Environ.* **2018**, *637–638*, 221–232. [[CrossRef](#)]
53. Chaudhry, H.; Vasava, H.B.; Chen, S.; Saurette, D.; Beri, A.; Gillespie, A.; Biswas, A. Evaluating the Soil Quality Index Using Three Methods to Assess Soil Fertility. *Sensors* **2024**, *24*, 864. [[CrossRef](#)]
54. Penn, C.; Camberato, J. A Critical Review on Soil Chemical Processes That Control How Soil pH Affects Phosphorus Availability to Plants. *Agriculture* **2019**, *9*, 120. [[CrossRef](#)]
55. Taaime, N.; El Mejahed, K.; Choukr-Allah, R.; Bouabid, R.; Oukarroum, A.; El Gharous, M. Optimization of Macronutrients for Improved Grain Yield of Quinoa (*Chenopodium quinoa* Willd.) Crop under Semi-Arid Conditions of Morocco. *Front. Plant Sci.* **2023**, *14*, 1146658. [[CrossRef](#)]
56. Akkacha, A.; Douaoui, A.; Younes, K.; El Sawda, C.; Alsyouri, H.; El-Zahab, S.; Grasset, L. Investigating the Impact of Salinity on Soil Organic Matter Dynamics Using Molecular Biomarkers and Principal Component Analysis. *Sustainability* **2025**, *17*, 2940. [[CrossRef](#)]

57. Matus, F.J. Fine Silt and Clay Content Is the Main Factor Defining Maximal C and N Accumulations in Soils: A Meta-Analysis. *Sci. Rep.* **2021**, *11*, 6438. [[CrossRef](#)] [[PubMed](#)]
58. Basak, N.; Rai, A.K.; Sundha, P.; Meena, R.L.; Bedwal, S.; Yadav, R.K.; Sharma, P.C. Assessing Soil Quality for Rehabilitation of Salt-Affected Agroecosystem: A Comprehensive Review. *Front. Environ. Sci.* **2022**, *10*, 935785. [[CrossRef](#)]
59. Parameswaran, T.G.; Sivapullaiah, P.V. Influence of Sodium and Lithium Monovalent Cations on Dispersivity of Clay Soil. *J. Mater. Civ. Eng.* **2017**, *29*, 04017042. [[CrossRef](#)]
60. Santos, P.D.D.; Cavalcante, L.F.; Gheyi, H.R.; Lima, G.S.D.; Gomes, E.M.; Bezerra, F.T.C. Saline-Sodic Soil Treated with Gypsum, Organic Sources and Leaching for Successive Cultivation of Sunflower and Rice. *Rev. Bras. Eng. Agríc. Ambient.* **2019**, *23*, 891–898. [[CrossRef](#)]
61. Xie, Y.; Ning, H.; Zhang, X.; Zhou, W.; Xu, P.; Song, Y.; Li, N.; Wang, X.; Liu, H. Reducing the Sodium Adsorption Ratio Improves the Soil Aggregates and Organic Matter in Brackish-Water-Irrigated Cotton Fields. *Agronomy* **2024**, *14*, 2169. [[CrossRef](#)]
62. Luiz, M.D.S.; Zanão Junior, L.A.; Ribeiro, M.R.; de Matos, M.A.; Andrade, D.S. Residual Effects of Agricultural Gypsum on Soil Chemical and Microbiological Characteristics. *Soil Use Manag.* **2022**, *38*, 1656–1666. [[CrossRef](#)]
63. Morsy, S.; Elbasyoni, I.S.; Baenziger, S.; Abdallah, A.M. Gypsum Amendment Influences Performance and Mineral Absorption in Wheat Cultivars Grown in Normal and Saline-Sodic Soils. *J. Agron. Crop Sci.* **2022**, *208*, 675–692. [[CrossRef](#)]
64. Cogo, F.D.; Saggin Júnior, O.J.; Guimarães, P.T.G.; Siqueira, J.O.; Carneiro, M.A.C. High Rates of Agricultural Gypsum Affect the Arbuscular Mycorrhiza Fungal Community and Coffee Yield. *Bragantia* **2020**, *79*, 612–622. [[CrossRef](#)]
65. Bolo, J.D.; Reynoso, A.; Cosme, R.C.; Arone, G.; Calderón, C. The Combined Application of Organic Fertilizers Improves the Physical Properties of Soil Associated to Quinoa (*Chenopodium quinoa* Willd.) Cultivation. *Sci. Agropecu.* **2020**, *11*, 401–408. [[CrossRef](#)]
66. Alvarez, R.; Evans, L.A.; Milham, P.J.; Wilson, M.A. Effects of Humic Material on the Precipitation of Calcium Phosphate. *Geoderma* **2004**, *118*, 245–260. [[CrossRef](#)]
67. Hitziger, M.; Ließ, M. Comparison of Three Supervised Learning Methods for Digital Soil Mapping: Application to a Complex Terrain in the Ecuadorian Andes. *Appl. Environ. Soil Sci.* **2014**, *2014*, 809495. [[CrossRef](#)]
68. Nozari, S.; Pahlavan-Rad, R.M.; Brungard, C.; Heung, B.; Boruvka, L. Digital Soil Mapping Using Machine Learning-Based Methods to Predict Soil Organic Carbon in Two Different Districts in the Czech Republic. *Soil Water Res.* **2024**, *19*, 32–49. [[CrossRef](#)]
69. Niaz, S.; Wehr, J.B.; Dalal, R.C.; Kopittke, P.M.; Menzies, N.W. Wetting and Drying Cycles, Organic Amendments, and Gypsum Play a Key Role in Structure Formation and Stability of Sodic Vertisols. *SOIL* **2023**, *9*, 141–154. [[CrossRef](#)]
70. Gonçalves Filho, F.; da Silva Dias, N.; Suddarth, S.R.P.; Ferreira, J.F.S.; Anderson, R.G.; dos Santos Fernandes, C.; de Lira, R.B.; Neto, M.F.; Cosme, C.R. Reclaiming Tropical Saline-Sodic Soils with Gypsum and Cow Manure. *Water* **2020**, *12*, 57. [[CrossRef](#)]
71. Yang, S.; Jansen, B.; Absalah, S.; van Hall, R.L.; Kalbitz, K.; Cammeraat, E.L.H. Lithology- and Climate-Controlled Soil Aggregate-Size Distribution and Organic Carbon Stability in the Peruvian Andes. *SOIL* **2020**, *6*, 1–15. [[CrossRef](#)]
72. Kong, J.; He, Z.; Chen, L.; Zhang, S.; Yang, R.; Du, J. Elevational Variability in and Controls on the Temperature Sensitivity of Soil Organic Matter Decomposition in Alpine Forests. *Ecosphere* **2022**, *13*, e4010. [[CrossRef](#)]
73. Peng, Y.; Sun, Y.; Fan, B.; Zhang, S.; Bolan, N.S.; Chen, Q.; Tsang, D.C.W. Fe/Al (Hydr)Oxides Engineered Biochar for Reducing Phosphorus Leaching from a Fertile Calcareous Soil. *J. Clean. Prod.* **2021**, *279*, 123877. [[CrossRef](#)]

**Disclaimer/Publisher’s Note:** The statements, opinions and data contained in all publications are solely those of the individual author(s) and contributor(s) and not of MDPI and/or the editor(s). MDPI and/or the editor(s) disclaim responsibility for any injury to people or property resulting from any ideas, methods, instructions or products referred to in the content.